Int. J. Solids Structures Vol. 24, No. 8, pp. 789–803, 1988
Printed in Great Britain.

0020-7683/88 $3.00 + .00

LOAD TRANSFER IN COMPOSITES WITH A COULOMB FRICTION INTERFACE

ANNA DOLLAR and PAUL S. STEIF
Department of Mechanical Engineering, Carnegie-Mellon University, Pittsburgh, PA 15213, U.S.A.

(*Received* 1 *September* 1987; *in revised form* 15 *March* 1988)

Abstract—The transfer of load across a frictional interface between elastic solids is investigated. We formulate a model two-dimensional problem in which a fiber is extracted from, or pressed into, a half-plane to which it is connected via Coulomb friction. With a continuous distribution of dislocations to represent the slip, this problem can be reduced to solving a singular integral equation. Results of interest are the extent of the slip zone, the transfer of load from the fiber to the matrix, and the amount by which the fiber is extracted or depressed, all of which depend on the load in a non-linear fashion. Attention is focused on contrasting the results of the present analysis with approximate treatments generally incorporated into micro-mechanical models of composite materials.

INTRODUCTION

Theories for the strength and toughness of fiber-reinforced composites have, for the most part, been based on rather simple assumptions regarding the way in which load is transferred between the fiber and the matrix. These theories (Kelly, 1970; Aveston *et al.*, 1971) typically assume that a constant shear stress acts at the fiber–matrix interface. This shear stress is often interpreted as the flow stress of the matrix or as the friction stress at the interface. Isolating the fiber and applying equilibrium then leads one to conclude that the average fiber stress varies linearly with distance along the fiber, the variation being proportional to the shear stress. Clearly, this means of analyzing load transfer is highly approximate; there is no accounting of compatibility or of the materials' constitutive behaviors, and there is only a global accounting of the equilibrium of one portion of the fiber. Actually, the shear stress at the interface is expected to equal the friction stress only over some portion of the fiber, and after that point it ought to decrease steadily with distance along the fiber. Moreover, as discussed below, the friction stress may not even be constant from point to point (as is usually assumed), but may depend on the normal stress. Nevertheless, this simple analysis of the distribution of fiber load constitutes an essential ingredient in most commonly used models for composite strength and toughness.

This paper is devoted to exploring the usefulness of this approximate method by comparing its predictions with the results of a more rigorous analysis. For this purpose, we contemplate a composite in which the fiber and the matrix are not bonded, and in which frictional slip can occur at their interface. Such interface conditions appear to prevail in composites of relatively brittle constituents, as exemplified by ceramic–matrix composites (Prewo and Brennan, 1980). Whether this interaction at the interface is caused by friction as it is usually thought of, or by mechanical keying or interlocking, it is plausible that the maximum shear stress that the interface can sustain increases with the prevailing normal pressure. In order to account for such a dependence in a simple fashion, we will consider the transfer of load across an interface which is described by Coulomb friction.

The simple load transfer analysis mentioned above is used, in particular, to describe the stresses near a fiber end, near a fiber break, or near a matrix crack. More generally, load transfer via shear stresses occurs whenever there is an interruption of the isostrain state which exists parallel to the fibers in a unidirectional, continuous fiber composite. To judge the accuracy of the simple, constant shear stress analysis described above, we consider a problem which exhibits this type of load transfer, and which is amenable to mathematical analysis. Specifically, we treat the problem of a two-dimensional pullout test, in which conditions at the fiber–matrix interface are those of Coulomb friction. Besides resembling

other load transfer processes which occur in loaded fiber composites, this configuration, or rather its three-dimensional generalization, is of interest in its own right. Pullout tests are a common means of assessing interface strength and micro-indentation tests (pressing on the fiber instead of pulling it out) have recently been suggested (Marshall, 1984) as a means of deducing the friction stress in ceramic–matrix composites. The two-dimensional pullout test addressed here has been studied previously (Steif and Hoysan, 1986) as a means of gauging the effect of an elastic interface on load transfer.

ANALYSIS

The model pullout test is shown schematically in Fig. 1. The half-plane occupying the region $y < 0$ is composed of three homogeneous, isotropic, elastic regions, $-\infty < x < -a$, $-a < x < a$, and $a < x < \infty$, all of which possess identical elastic constants G and ν. Interface conditions along $x = \pm a$ are described by a pointwise Coulomb friction law. According to this friction law, at any instant in the loading history, either sticking, slipping, or opening occurs at a generic point along the interface. Conditions for these three states along $x = a$ are as follows:

stick condition

$$\sigma < 0, \quad |\tau| < \mu|\sigma|, \quad \frac{dg}{dt} = 0, \quad h = \frac{dh}{dt} = 0 \tag{1a}$$

slip condition

$$\sigma < 0, \quad |\tau| = \mu|\sigma|, \quad \operatorname{sgn}\left(\frac{dg}{dt}\right) = \operatorname{sgn}(\tau), \quad h = \frac{dh}{dt} = 0 \tag{1b}$$

open condition

$$\sigma = \tau = 0, \quad h > 0 \tag{1c}$$

with

$$\sigma = \sigma_{xx}, \quad \tau = \sigma_{xy}$$

$$g = \lim_{\varepsilon \to 0^+} [v(a+\varepsilon, y) - v(a-\varepsilon, y)]$$

$$h = \lim_{\varepsilon \to 0^+} [u(a+\varepsilon, y) - u(a-\varepsilon, y)].$$

In these equations σ_{xx} and σ_{xy} denote the usual Cartesian components of stress, u and v denote the x- and y-components of displacement, respectively, μ the friction coefficient which is assumed to be constant along the interface, and $d(\ )/dt$ the derivative with respect to a time-like parameter that increases monotonically as loading proceeds. The condition

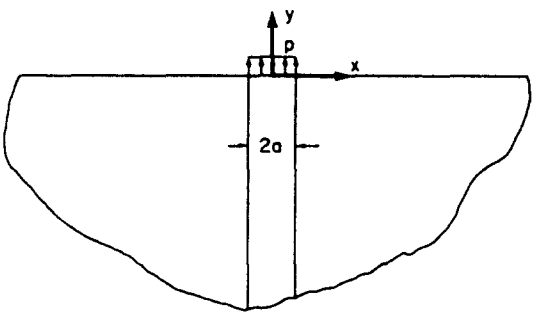

Fig. 1. Schematic of two-dimensional pullout test.

$\mathrm{sgn}(\mathrm{d}g/\mathrm{d}t) = \mathrm{sgn}(\tau)$ is the condition of positive energy dissipation which dictates that the instantaneous increment of slip be in the same direction as the shear stress. Note that we ignore the distinction between static and kinetic friction.

To simulate the presence of some pre-existing compression at the interface (possibly arising from differential thermal strains that occur during processing), a uniform lateral compression $\sigma_{xx} = -\sigma_0 (\sigma_0 > 0)$ is imposed on the half-plane. Finally, the half-plane is subjected to a uniform normal traction p applied along $-a < x < a, y = 0$.

An integral equation governing this problem is now derived in a manner similar to that used previously (Steif and Hoysan, 1986). The solution to a normally loaded, perfectly bonded half-plane is superposed with a distribution of edge dislocations along $x = \pm a$. Symmetry requires that the dislocations be equal and opposite along $x = a$ and $-a$. The kernel solution one requires is that of a dislocation in an elastic half-plane (Hirth and Lothe, 1967). This solution can be written succinctly in terms of Muskhelishvili's (1963) complex stress potentials ϕ and ψ, which are related to the Cartesian components of stress and displacement according to

$$\sigma_{xx} + \sigma_{yy} = 2(\phi' + \overline{\phi'}) \tag{2a}$$

$$\sigma_{yy} - \sigma_{xx} + 2\mathrm{i}\sigma_{xy} = 2(\bar{z}\phi'' + \psi') \tag{2b}$$

$$2G(u + \mathrm{i}v) = \kappa\phi - z\overline{\phi'} - \overline{\psi} \tag{2c}$$

where ϕ and ψ are sectionally holomorphic functions of $z = x + \mathrm{i}y$, G the elastic shear modulus, $\kappa = 3 - 4\nu$ in plane strain (ν is Poisson's ratio), $(\ )'$ denotes differentiation with respect to z, and the overbar denotes complex conjugation.

The solution for the dislocation in the half-plane is

$$\phi' = \frac{\alpha}{z - z_0} + \frac{\bar{\alpha}(\bar{z}_0 - z_0)}{(z - \bar{z}_0)^2} - \frac{\alpha}{z - \bar{z}_0} \tag{3a}$$

$$\psi' = \frac{\bar{\alpha}}{z - z_0} + \frac{\alpha\bar{z}_0}{(z - z_0)^2} - \frac{\bar{\alpha}}{z - \bar{z}_0} - \frac{\bar{\alpha}(z_0 - \bar{z}_0)(z + \bar{z}_0)}{(z - \bar{z}_0)^3} - \frac{\alpha\bar{z}_0}{(z - \bar{z}_0)^2} \tag{3b}$$

where α is given by

$$\alpha = \frac{G(-\mathrm{i}b_x + b_y)}{(\kappa + 1)\pi}.$$

For an extensive range of loading and material parameters, no opening occurs at the interface, which means that $b_x = 0$. In this paper we only consider situations in which $b_x = 0$, although we will point out circumstances in which the zero opening condition is violated. Thus, only dislocations b_y are distributed over the portions of the interface on which slip occurs. Let the shear stress be written in the form $\tau = \tau_p + \tau_d$ and the normal stress in the form $\sigma = -\sigma_0 + \sigma_p + \sigma_d$, where τ_p and σ_p are the stresses due to the normal loading of the perfectly bonded half-plane, and τ_d and σ_d are the stresses due to the distributed dislocations. Then, the slip condition, given by $\tau = \pm\mu|\sigma|$, leads to the integral equation

$$\tau_p(\xi) + \int_\Gamma H_\tau(\xi, \eta) b(\eta)\, \mathrm{d}\eta = \pm\mu \left| -\sigma_0 + \sigma_p(\xi) + \int_\Gamma H_\sigma(\xi, \eta) b(\eta)\, \mathrm{d}\eta \right| \tag{4}$$

where $\xi = -y/a$, and $b(\eta)$ is the dislocation density b_y at $y = -\eta a$. The kernels H_τ and H_σ give the shear stress and normal stress, respectively, at $x = a, y = -a\xi$ due to a unit positive dislocation at $x = a, y = -a\eta$ and a unit negative dislocation at $x = -a, y = -a\eta$. The terms τ_p and σ_p are given by

$$\tau_p(\xi) = \frac{-4p}{\pi[\xi^2+4]}, \quad \sigma_p(\xi) = \frac{p}{\pi}\left[\frac{\pi}{2} - \tan^{-1}\frac{\xi}{2} - \frac{2\xi}{\xi^2+4}\right]. \tag{5a, b}$$

Expressions for the kernels H_τ and H_σ are given in the Appendix.

The interval Γ over which eqn (4) is defined is part of the solution, as is the sign to be taken for the right-hand side. Provided no opening occurs, eqn (4) describes the frictional slip resulting from monotonic loading. When unloading takes place, it is necessary to augment the expressions for τ and σ to include terms reflecting the residual (locked-in) stresses arising from previous slip. Then, the dislocation density may be interpreted as associated with further slip. The irreversibility of the frictional slip makes the solution to this problem loading-history dependent; we will solve the problem for the simple history of monotonic loading and then unloading. The evolution of the slip and the slipping zone will be discussed below.

Many of the subtleties associated with Coulomb friction at an interface between elastic solids have been discussed by Dundurs and Comninou (1979, 1981) and Comninou and Dundurs (1982). In particular, they show that the condition that the friction law be nowhere violated implies that the stresses remain nonsingular; from this it may be inferred that the dislocation density vanishes at the ends of a slipping zone. The integral equation must then be supplemented by the consistency condition (Muskhelishvili, 1977), which provides an additional equation for finding the unknown length of the slip zone. The integral equation was solved numerically using a method developed by Erdogan *et al.* (1973).

RESULTS AND DISCUSSION

Much insight into the results can be gained by simply considering the distributions of interfacial shear and normal traction due to the normal loading of the perfectly bonded half-plane. The distributions of τ_p and σ_p are given in eqns (5), and they have been sketched in Fig. 2 along with τ_p/σ_p.

One can immediately appreciate that the cases of $p > 0$ (initial tensile loading) and $p < 0$ (initial compressive loading) are quite different. In both cases, the normal stress and the shear stress induced by the load p are greatest in magnitude at $y = 0$. In the case of applied tension, the normal stress σ_p is tensile at the interface. This tensile stress serves to diminish the prevailing compressive stress, thereby lessening the frictional resistance most

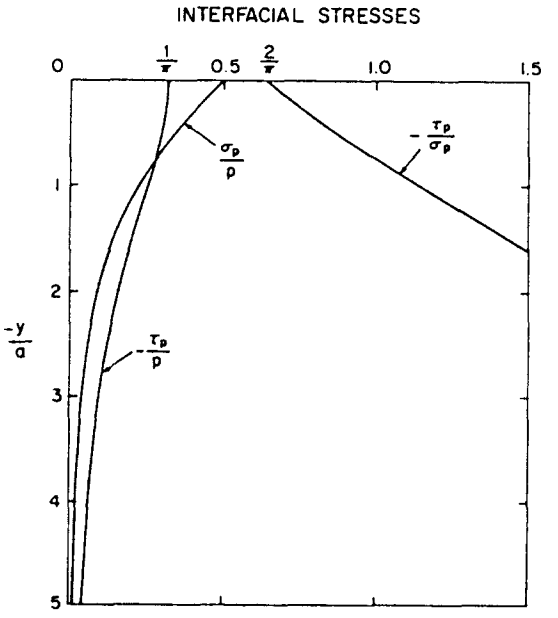

Fig. 2. Interfacial stresses associated with normal loading of perfectly bonded half-plane.

at $y = 0$ where the shearing stress is greatest. Using eqns (5), one finds that, under an applied tension, slip begins at $y = 0$ at a tension of

$$p^* = \frac{2\pi\mu\sigma_0}{2+\pi\mu}. \tag{6}$$

When $p < 0$, the interfacial normal stress σ_p is compressive. Thus, the farther one goes into the solid, the less is the frictional resistance $\mu|-\sigma_0+\sigma_p|$; the shear stress decreases likewise. The precise distributions of τ_p and σ_p lead to slip initiating at a point y^* inside the half-plane which is given by

$$y^* = -2a\mu \tag{7}$$

at a pressure

$$p^* = \frac{-\pi\mu\sigma_0}{1-\mu\tan^{-1}(1/\mu)}. \tag{8}$$

The progression of slip is also different as the load is increased. For applied tension, slip spreads monotonically into the solid. On the other hand, the slip zone spreads in both directions (into the solid and up to the surface) in the case of applied compression. Once it reaches the surface, the slip zone then spreads monotonically into the solid.

In Fig. 3, the locations of the end points of the slip zone are plotted as a function of the load p, normalized by σ_0. For $p > 0$, the interpretation is straightforward. To interpret the curves for $p < 0$, consider, for example, the curve labeled $\mu = 0.7$. Slip begins at $y = -1.4a$ when $p/\sigma_0 = -6.71$. When $p/\sigma_0 = -7.0$, slip extends from $y = -0.941a$ to $-1.975a$. The slip zone reaches the surface when $p/\sigma_0 = -10.5$. Generally speaking, the results in Fig. 3 are not unexpected: the extent of slip increases with increasing load and diminishing friction coefficient. The curves depicting the slip length for tension are ended abruptly at the points shown when the interfacial normal stress becomes zero. Under further loading the normal stress changes sign, clearly violating the condition $\sigma \leqslant 0$. This indicates that opening occurs at the interface when these levels of applied tension are reached. While

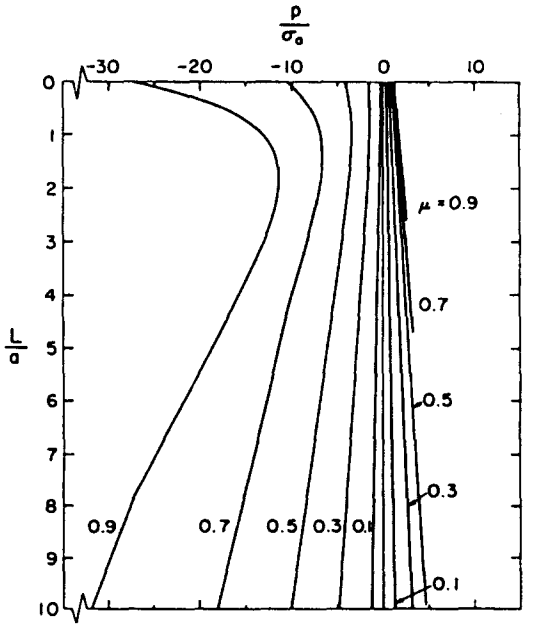

Fig. 3. End points of slip zone as a function of normalized load p/σ_0.

the consequences of opening are undoubtedly of interest, they are not pursued further here. Note that no opening occurs under compressive loading.

Consider now applying the simple analysis described in the Introduction to the two-dimensional pullout test analyzed here. We assume the slip extends from the surface to the point $y = -L_{app}$. The simple analysis involves a constant interfacial shear stress. An obvious choice for this is the quantity $\mu\sigma_0$, which would be the friction stress remote from the region of loading. With this choice, the simple analysis yields the result

$$\frac{L_{app}}{a} = \frac{|p|}{\mu\sigma_0}. \tag{9}$$

Note the approximate analysis predicts that the slip length depends on the friction coefficient only through the nominal friction stress $\mu\sigma_0$. The form of this approximate result suggests a different normalization of the results based on the Coulomb friction law. Accordingly, the slip length is replotted as a function of $p/\mu\sigma_0$ in Fig. 4. The dashed lines represent the approximate solution, which is independent of μ, given this normalization, and which gives identical predictions for tension and compression. Thus, Fig. 4 serves to highlight the distinction between the simple constant shear stress approximation and the solution based on a Coulomb friction interface.

Indeed, the two most striking features of the Coulomb friction model are the clear variation with μ, even after the normalization, and the marked distinction between tensile and compressive loading of the fiber. First, not surprisingly, the slip lengths are much greater for tension than for compression. More interesting is the difference in the effect of changes in μ on the slip length. For fixed $|p/\mu\sigma_0|$, increasing μ decreases the slip length when $p < 0$, while the slip increases with μ when $p > 0$. This is partially explained by noting that fixing $p/\mu\sigma_0$ means that higher values of μ imply higher values of $|p|$, which give rise to higher load induced interfacial normal stresses. When $p < 0$, these augment the pre-existing compression, but when $p > 0$, the normal stresses are tensile, thereby diminishing the friction stress. Additionally, one notices here a trend which will be observed throughout this study: the results of the approximate analysis approach the results based on the Coulomb friction interface in the limit as $\mu \to 0$ with $\mu\sigma_0$ held constant.

The explanation for the validity of the approximate analysis in the limit of small friction coefficients is straightforward. The results based on the pointwise Coulomb friction

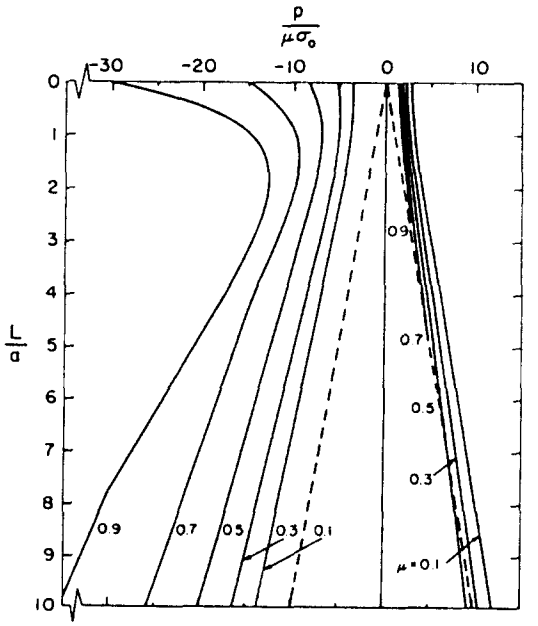

Fig. 4. End points of slip zone as a function of normalized load $p/\mu\sigma_0$: ---, constant shear stress approximation.

law differ from the approximate results because the normal stress at the interface is altered from the value σ_0 by the stresses associated with the loading (σ_p) and by stresses generated by dislocations (seen below to be small). The difference between the two theories, therefore, depends on the level of the stresses associated with loading relative to σ_0. To lowest order, the loading required to cause slip depends on $\mu\sigma_0$, and so do the stresses. On the other hand, for a fixed value of $\mu\sigma_0$, σ_0 must be relatively large if μ becomes small. Thus, in this limit, the stresses associated with loading are small compared with σ_0, bringing the two theories into close agreement.

A significant ingredient in theories for the tensile failure of fiber composites is the rate at which load is transferred from the fiber to the matrix, or vice versa. Load transfer is depicted in Fig. 5, where we have plotted Σ, the average stress σ_{yy} across the fiber, normalized by p, as a function of normalized distance into the composite. The normalized load has been fixed at $|p/\mu\sigma_0| = 10$. Curves signifying tensile loading are labeled $p > 0$; $p < 0$ denotes compressive loading. For purposes of comparison, we also exhibit the load transfer as it is predicted by the highly approximate theory outlined in the Introduction. In this approximate theory, a constant shear stress (taken here to be $\mu\sigma_0$) acts at the interface. This implies that the average fiber stress varies linearly (the dashed line in Fig. 5) from the applied value p at the surface to a value of 0 at $y = -L_{app}$, given in eqn (9). The dotted line represents load transfer when the fiber and the matrix are perfectly bonded.

Consider the range over which 80% of the load is transferred; i.e. $0.2 < \Sigma/p < 1.0$. (Obviously, the approximate solution is completely inaccurate when, say, the final 10% of the load diffuses out, since it assumes that *all* the load diffuses out over a *finite distance*.) As in the case of the slip length, there are marked variations with μ and the results for tensile and compressive loading are different. Consistent with intuition, the load diffuses more slowly in tension (the pre-existing interfacial compression is relieved by the load-induced normal stress) and more quickly in compression. To show the effect of increasing load, we depict the load diffusion for $p/\mu\sigma_0 = -35$ (Fig. 6). A comparison of Figs 5 and 6 indicates that the deviations from the approximate solution increase with the load. This holds for tension as well, although our solution has not been extended to permit large values of tensile loading for which opening at the interface occurs.

For practical composites, $p/\mu\sigma_0$ is conceivably of the order of 100–600. Hence, we consider further the dependence of load diffusion on the magnitude of p for compression. If the curves for different values of $p/\mu\sigma_0$ were plotted as before (Fig. 5) as a function of y/a, then

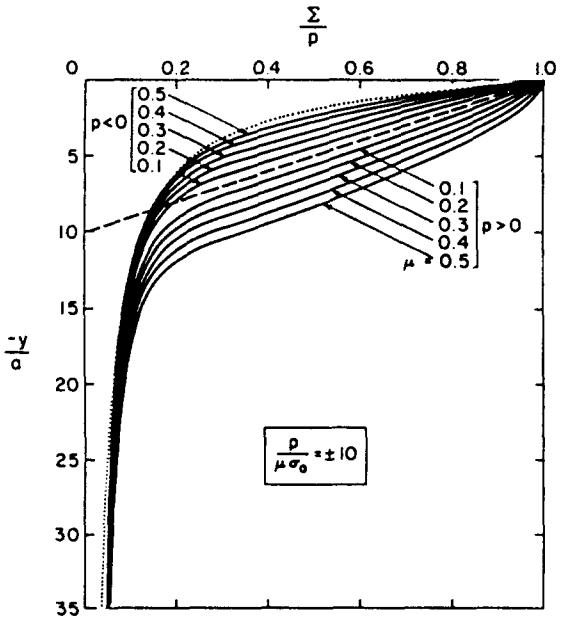

Fig. 5. Load transfer for tensile and compressive loadings ($p/\mu\sigma_0 = \pm 10$): - - -, constant shear stress approximation; · · ·, perfectly bonded interface.

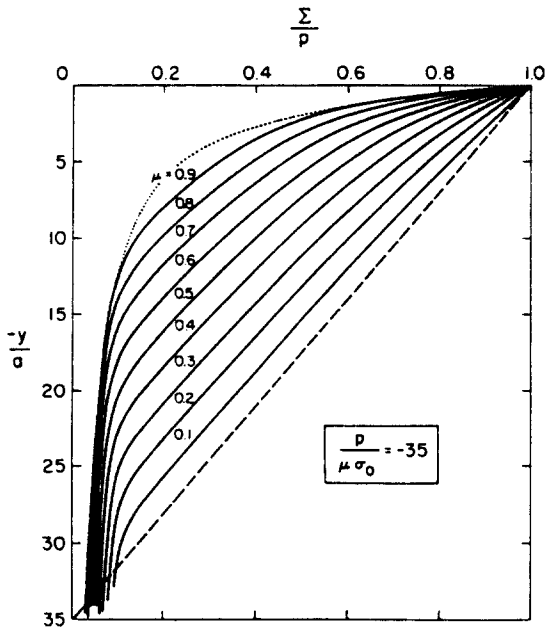

Fig. 6. Load transfer for compressive loading ($p/\mu\sigma_0 = -35$): ---, constant shear stress approximation; · · ·, perfectly bonded interface.

there would be a different approximate curve for each level of load. To compare these results, we renormalize the distance into the composite by the slip length, eqn (9), as calculated by the approximate theory (Fig. 7). Now, for all combinations of parameters, the load diffusion as predicted by the approximate theory is the dashed line of slope 1. Consider the curves that are labeled with different values of $p/\mu\sigma_0$ ($\mu = 0.2$). Note that the curves appear to approach a limiting curve as $p/\mu\sigma_0 \to \infty$. Also depicted in Fig. 7 are the curves for $\mu = 0.6$. The results suggest a universal normalization, dependent only on μ, of the load transfer curves for large compressive loads.

We now turn to consider the fiber depression, a quantity which is central to the microindentation test. The slip at the surface $g(0)$, normalized by $ap(\kappa+1)/G$ is plotted as a

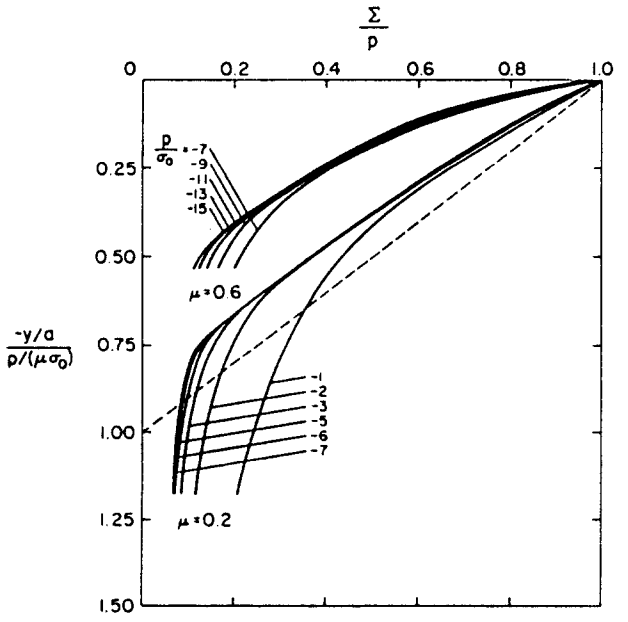

Fig. 7. Load transfer as a function renormalized distance for compressive loading: ---, constant shear stress approximation.

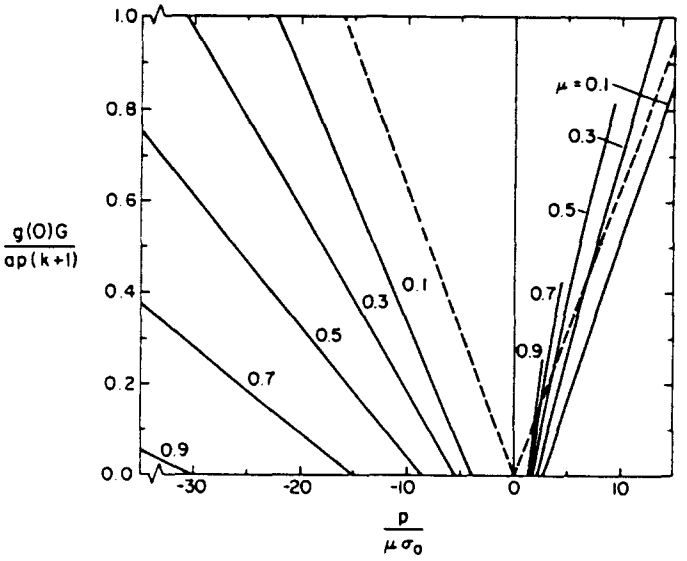

Fig. 8. Slip at the surface for tensile and compressive loadings as a function of renormalized load $p/\mu\sigma_0$: ---, constant shear stress approximation.

function of the normalized load $p/\mu\sigma_0$ in Fig. 8. Of course, applied compression causes a depression, while tension produces an extraction. One can similarly employ the approximate analysis (constant interfacial shear stress model) to analyze the fiber depression. This is essentially the analysis used by Marshall (1984) and Marshall and Evans (1985) to model their micro-indentation test. In this analysis, the linear load transfer gives a linear variation of strain which is integrated along the slip length to give the slip at the surface g_{app}. For plane strain, g_{app} is given by

$$\frac{g_{app}G}{ap(\kappa+1)} = \frac{p}{16\mu\sigma_0}. \tag{10}$$

Equation (10) is plotted as the dashed lines in Fig. 8.

Though the approximate solution indicates no difference between tension and compression, the solution to the Coulomb friction problem indicates that they are markedly different. Note the difference between the approximate solution and the actual results for compression. Both the slopes of the curves and the load at which slip begins vary significantly with μ. A quantitative comparison can be made for, say $p/\mu\sigma_0 = 500$ (a typical value in Marshall and Evans (1985), assuming their inferred value of the friction stress). The approximate result is $g_{app}G/[ap(\kappa+1)] = 31.25$, while our numerical solution yields $g(0)G/[ap(\kappa+1)] = 16.5$ for $\mu = 0.4$.

In passing, we note a physical interpretation for the extraction when $p > 0$. When a matrix crack normal to the loading direction traverses a longitudinally loaded, unidirectional composite, the shift of load from the matrix to the fiber corresponds to a tensile load applied to the fiber. Thus, the extraction corresponds roughly to the interfacial slip accompanying a matrix crack. The present results suggest that one exercise caution in using the approximate solution for the friction dissipation which enters energy based criteria for matrix cracking (Aveston *et al.*, 1971; Aveston and Kelly, 1973; Budiansky *et al.*, 1986). In fact, the difference between the approximate solution and the solution based on a Coulomb friction model is likely to be even greater when allowance is made for the gap which opens up between the fiber and the matrix.

We turn now to the response of the half-plane to monotonic loading followed by monotonic unloading. The progression of slip is somewhat more complicated than it was for loading, and different behaviors upon initial unloading allow one to draw the distinction between strong friction and weak friction, a distinction discussed previously by Dundurs

and Comninou (1981). Before presenting numerical results, we first discuss in very general terms the response to initial unloading.

Consider the case of loading in compression ($p < 0$) to some maximum load followed by an application of a small tension (initial unloading). Let τ_r and σ_r denote the values of τ and σ at the maximum load. (As mentioned earlier, these residual stresses must be included in the left- and right-hand sides of eqn (4); then, the dislocation distribution $b(\eta)$ represents additional slip occurring after the maximum load has been reached.) Note that $\tau_r > 0$ and $\sigma_r < 0$ and, in particular, that $\tau_r = -\mu\sigma_r$ in $-L < y < -L_0$, where L and L_0 denote the end points of the slipped region. (Once slip reaches the surface $L_0 = 0$.) Let τ_t and σ_t be the additional shear and normal stress induced by the tensile unloading.

We now explore conditions under which no additional slippage occurs with unloading, i.e. conditions under which

$$\tau < -\mu\sigma$$

where we have assumed that τ is still positive and σ is still negative. This equality can be written as

$$\tau_r + \tau_t < -\mu(\sigma_r + \sigma_t)$$

and rearranged in the form

$$\tau_r + \mu\sigma_r < -\tau_t - \mu\sigma_t.$$

Since we assumed that no additional slip occurs, τ_t and σ_t are given by eqns (5) which are pertinent to the perfectly bonded half-plane loaded in tension, whence $\tau_t < 0$ and $\sigma_t > 0$. Now, define the function $f(\xi)$ by

$$f(\xi) = -\frac{\tau_t}{\sigma_t} \tag{11}$$

implying

$$\tau_r + \mu\sigma_r < \sigma_t[f(\xi) - \mu]. \tag{12}$$

The function $f(\xi)$, shown in Fig. 2, has a minimum value of $2/\pi$ at $\xi = 0$.

In the region $-L < y < -L_0$, $\tau_r + \mu\sigma_r = 0$; hence, inequality (12) reduces to

$$f(\xi) - \mu > 0.$$

Two ranges of μ emerge: $\mu < 2/\pi$, which we term "weak friction", and $\mu > 2/\pi$, which we term "strong friction". For weak friction, the inequality is satisfied, and our assumption that $-\tau_t/\sigma_t$ can be calculated from eqns (5) is consistent with the fact that no additional slippage occurs. Note also that $\tau_r < -\mu\sigma_r$ in the ranges $-\infty < y < -L$ and $-L_0 < y < 0$; this implies that upon initial unloading, slip will also not occur in previously unslipped regions provided $\mu < 2/\pi$. Once unloading has occurred to a sufficient extent, it is possible for reverse slip to occur, that is, the tensile unloading begins to draw the fiber back up. This takes place, of course, only after the sign of the shear stress reverses and becomes negative. If the maximum initial loading is sufficiently large, reverse slip will occur; for small initial loadings, complete tensile unloading is accompanied by no reverse slip. When it does occur, reverse slip begins slightly below the surface and advances into the solid and up to the surface, consistent with the Dundurs and Comninou (1981) definition of weak friction. We return to reverse slip below.

When $\mu > 2/\pi$, the right-hand side of inequality (12) is negative for some range of ξ. Thus, depending on how much slip has occurred in loading, inequality (12) may be violated,

meaning that slip may occur immediately upon unloading. If the slip zone has reached the surface during loading, then such slip will certainly take place. What is interesting is that initial tensile unloading with strong friction causes the fiber to slip *further into* the matrix. This is dictated by the positive dissipation condition that the slip be in the same direction as the shear stress, which is still positive for sufficiently small unloading. The interpretation is as follows: unloading with strong friction causes a release of compressive stress at the interface which is sufficient to balance the decrease in the prevailing shear stress. This further slip initiates in some zone $-L_f < y < 0$, which then recedes to the surface with continued unloading, consistent with the Dundurs and Comninou (1981) definition of strong friction.

The case of initial tensile loading followed by compressive unloading is treated in the same manner. The result is the inequality

$$-\tau_r+\mu\sigma_r < -\sigma_c[f(\xi)+\mu]$$

where $\sigma_c < 0$ is the normal stress for compressive loading. Note that

$$-\tau_r+\mu\sigma_r \leqslant 0$$

from which it can be concluded that there cannot be continued slip upon initial compressive unloading for any value of μ.

We turn now to consider whether complete unloading is possible with no reverse slip. Let there be an initial compressive loading. Since reverse loading would occur when $\tau < 0$, the condition of zero reverse slip is

$$-\tau < -\mu\sigma.$$

Upon complete unloading, τ_p and σ_p both vanish. This means that $\tau = \tau_d$ and $\sigma = -\sigma_0+\sigma_d$ where τ_d and σ_d are the stresses due to slip (associated with the distributed dislocations) during initial loading. Hence, the condition for no reverse slip is

$$\tau_d-\mu\sigma_d+\mu\sigma_0 > 0. \tag{13}$$

For sufficiently small initial loading, relatively little slip occurs, implying that τ_d and σ_d are small. The condition then reduces to $\sigma_0 > 0$, which is always satisfied. From the numerical solution the terms $\tau_d-\mu\sigma_d$ are found to be negative. Hence, with sufficient initial loading, reverse slip must occur upon unloading.

Corresponding to initial tensile loading, the zero reverse slip condition is

$$-\tau_d-\mu\sigma_d+\mu\sigma_0 > 0 \tag{14}$$

and, again, it may be concluded that no reverse slip takes place upon unloading only when the initial tensile load is small.

The extent of reverse slip upon complete unloading, denoted by L_{un}, can be seen in Fig. 9. The curves for $p/\sigma_0 < 0$ refer to unloading from initial compression; $p/\sigma_0 > 0$ represents unloading from initial tension. Analogously to initial loadings, there is a range of maximum compressive loadings for which reverse slip occurs only internally. With reference to inequality (13), this is because for some range of initial compressive loadings, τ_d achieves an algebraic minimum not at $y = 0$ but at some interior point, and the reverse slip which begins at that point does not reach the surface. On the other hand, reverse slip that takes place upon unloading from tension always initiates at the surface. Reverse slip at the surface is depicted in Fig. 10, where for comparison both loading and unloading curves are shown. Consider, for example, the curve labeled $\mu = 0.5$ ($p/\mu\sigma_0 < 0$). When loading up to $p/\mu\sigma_0 > -13.4$, there is no reverse slip. Say the initial loading is to $p/\mu\sigma_0 = -35.0$; the normalized depression upon initial loading is 0.75 (dashed curve).

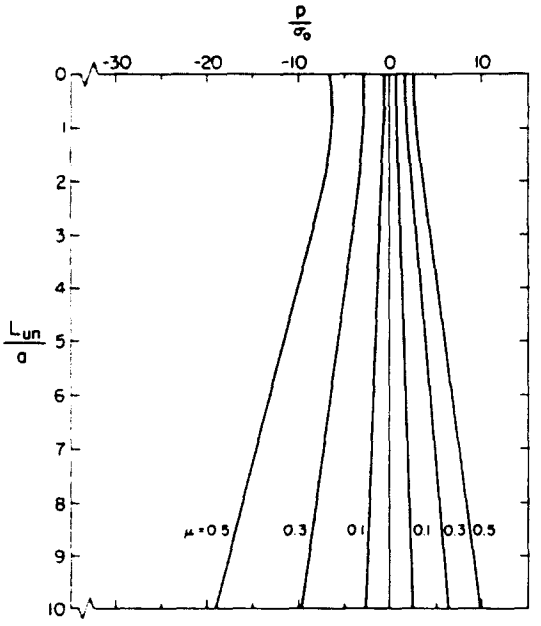

Fig. 9. End points of reverse slip zone as a function of normalized load p/σ_0.

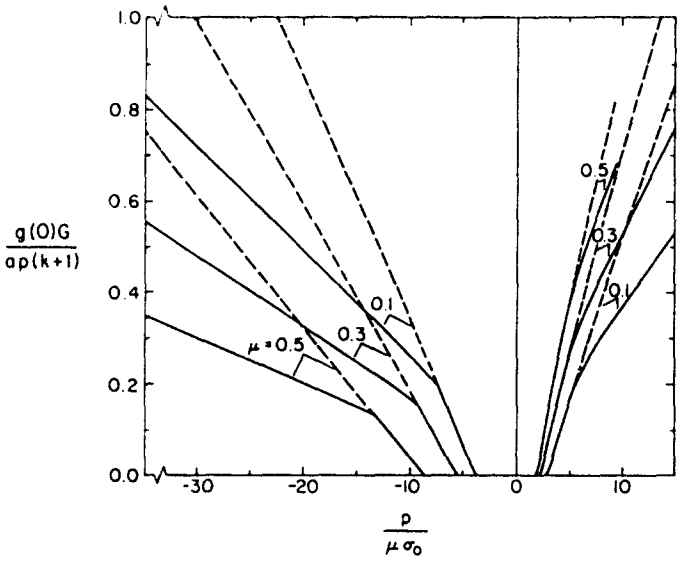

Fig. 10. Slip (dashed curves) and reverse slip (solid curves) at the surface for tensile and compressive loadings as a function of renormalized load $p/\mu\sigma_0$.

Upon complete unloading, the residual depression is 0.35 (solid curve); the amount of reverse slip is the difference 0.4.

Finally, we derive an approximate expression for the slip length under compressive loading which is asymptotically valid for $L/a \to \infty$. Consider the equilibrium of the section of the fiber over which slip occurs. The average pressure at $y = 0$ is p; let the average pressure at the end of the slip zone be p_0 (now we are taking p and p_0 to be positive). This net force downwards is balanced by distributed shear stresses, i.e.

$$(p-p_0)a = \int_{-L}^{0} \tau \, dy = \mu \int_{-L}^{0} |\sigma| \, dy \tag{15}$$

or

$$(p-p_0)a = \mu\sigma_0 L - \mu\int_{-L}^{0} \sigma_p \, dy - \mu\int_{-L}^{0} \sigma_d \, dy. \tag{16}$$

Note that

$$\int_{-x}^{0} \sigma_d \, dy = 0$$

and, thus, the last integral can be neglected in this asymptotic solution. That the numerical solutions indicate

$$\int_{-L}^{0} \sigma_d \, dy \approx 0$$

for even moderate values of L/a suggests that this approximate solution is reasonably accurate for finite values of L/a.

The first integral in eqn (16) is readily evaluated to give

$$\int_{-L}^{0} -\sigma_p \, dy = \frac{p}{\pi} L\left[\frac{\pi}{2} + \tan^{-1}\left(\frac{-L}{2a}\right)\right]$$

where, again $p > 0$. Letting $q(L/a)$ be defined by

$$q(L/a) = \frac{L}{a}\left[\frac{\pi}{2} + \tan^{-1}\left(\frac{-L}{2a}\right)\right]$$

one can write eqn (16) in the form

$$\frac{p}{\mu\sigma_0} = \frac{\dfrac{L}{a} + \dfrac{p_0}{\mu\sigma_0}}{1 - \dfrac{\mu}{\pi} q(L/a)}. \tag{17}$$

Neglecting $p_0/\mu\sigma_0$ in comparison with L/a, and noting that $q(L/a) \to 2$ for $L/a \to \infty$, one sees that eqn (17) reduces to

$$\frac{L}{a} = \frac{p}{\mu\sigma_0}\left(1 - \frac{2\mu}{\pi}\right). \tag{18}$$

This result is tabulated in Table 1, along with an extrapolation of the numerical results based on two values of L/a, both of the order of 10. The asymptotic result, eqn (18), agrees reasonably well with the numerical results. As observed earlier, the approach that assumed a constant interfacial shear stress and which led to eqn (9), becomes valid as $\mu \to 0$.

Table 1. Coefficient c in $L/a = c(p/\mu\sigma_0) + d$ from compressive loading

μ	0.1	0.2	0.3	0.4	0.5	0.6	0.7	0.8	0.9
Numerical	−0.877	−0.811	−0.748	−0.686	−0.627	−0.569	−0.510	−0.459	−0.411
Asymptotic result, eqn (18)	−0.936	−0.873	−0.809	−0.745	−0.682	−0.618	−0.554	−0.491	−0.427

Furthermore, eqn (18) also suggests that at $\mu = \pi/2$, the slip zone can no longer penetrate to arbitrary depths, though eqn (8) shows that slip will always initiate at some pressure p, for all finite values of μ. In fact, a careful examination of the numerical results revealed that the slope of L/a vs $p/\mu\sigma_0$ decreases steadily with increasing μ, apparently approaching zero near $\mu = \pi/2$. Since such high values of the friction coefficient appear not to be realistic, this was not pursued further.

CONCLUSIONS

The principal conclusion of this study is that using a constant shear stress model for a fiber–matrix interface which is actually governed by Coulomb friction may lead to substantially inaccurate results. This constant shear stress approximation, which underlies most calculations of composite strength and toughness, neglects differences between tensile and compressive loads on the fiber, which can be significant. Generally, the constant shear stress approximation overestimates the amount and extent of slip when the fiber is subjected to compression, while underestimating these quantities when the fiber is subjected to tension. Furthermore, it was found that the degree to which the constant shear approximation is in error increases with the friction coefficient and the load. Thus, depending on the actual value of the friction coefficient, the approximate calculation used by Marshall and Evans (1985) to analyze their micro-indentation test may be somewhat inaccurate. The approximate calculation is also likely to overestimate the rate at which the load is shed back to the matrix in the vicinity of a matrix crack. In fact, when the fiber is subjected to a sufficient level of tensile loading, a gap develops between the fiber and the matrix. This can extend the length over which the fiber load is enhanced following the development of a matrix crack.

Acknowledgements—The authors are grateful to Professor C. Y. Hui for a critical reading of the manuscript. This work has been supported by the National Science Foundation under grant MSM-8451080, by the General Electric Engine Business Group, by the Alcoa Technical Center, and by the Department of Mechanical Engineering, Carnegie-Mellon University.

REFERENCES

Aveston, J. and Kelly, A. (1973). Theory of multiple fracture of fibrous composites. *J. Mater. Sci.* **8**, 352.

Aveston, J., Cooper, G. A. and Kelly, A. (1971). The properties of fibre composites. In *Conference Proceedings, National Physical Laboratory*, p. 15. IPC Science and Technology Press, Guildford.

Budiansky, B., Hutchinson, J. W. and Evans, A. G. (1986). Matrix fracture in fiber-reinforced ceramics. *J. Mech. Phys. Solids* **34**, 167.

Comninou, M. and Dundurs, J. (1982). An educational elasticity problem with friction. Part 2: unloading for strong friction and reloading. *J. Appl. Mech.* **49**, 47.

Dundurs, J. and Comninou, M. (1979). Some consequences of the inequality conditions in contact and crack problems. *J. Elasticity* **9**, 71.

Dundurs, J. and Comninou, M. (1981). An educational elasticity problem with friction. Part 1: loading and unloading for weak friction. *J. Appl. Mech.* **48**, 841.

Erdogan, F., Gupta, G. D. and Cook, T. S. (1973). Numerical solution of singular integral equations. In *Mechanics of Fracture 1. Methods of Analysis and Solutions of Crack Problems* (Edited by G. C. Sih). Noordhoff, The Netherlands.

Hirth, J. P. and Lothe, J. (1967). *Theory of Dislocations*. McGraw-Hill, New York.

Kelly, A. (1970). Interface effects and the work of fracture of a fibrous composite. *Proc. R. Soc. Lond.* **A319**, 95.

Marshall, D. B. (1984). An indentation method for measuring matrix fiber frictional stresses in ceramic composites. *J. Am. Ceram. Soc.* December, C-259.

Marshall, D. B. and Evans, A. G. (1985). Failure mechanisms in ceramic fiber ceramic matrix composites. *J. Am. Ceram. Soc.* **68**, 225.

Muskhelishvili, N. I. (1963). *Some Basic Problems of the Mathematical Theory of Elasticity*. Noordhoff, The Netherlands.

Muskhelishvili, N. I. (1977). *Singular Integral Equations*. Noordhoff, The Netherlands.

Prewo, K. M. and Brennan, J. J. (1980). High-strength silicon carbide fibre-reinforced glass matrix composites. *J. Mater. Sci.* **15**, 463.

Steif, P. S. and Hoysan, S. F. (1986). On load transfer between imperfectly bonded constituents. *Mech. Mater.* **5**, 375.

APPENDIX

$$H_c = \frac{G}{(\kappa+1)\pi}[R_0(\xi,\eta)+R_1(\xi,\eta)]$$

$$H_o = \frac{G}{(\kappa+1)\pi}R_2(\xi,\eta)$$

where

$$R_0(\xi,\eta) = \frac{2}{\eta-\xi}$$

$$R_1(\xi,\eta) = \frac{2[4-(\xi-\eta)^2](\eta-\xi)}{[4+(\xi-\eta)^2]^2}+F_1(1+i\xi,1+i\eta)-F_1(1+i\xi,-1+i\eta)$$

$$R_2(\xi,\eta) = -\frac{4[4-(\xi-\eta)^2]}{[4+(\xi-\eta)^2]^2}+F_2(1+i\xi,1+i\eta)-F_2(1+i\xi,-1+i\eta)$$

$$F_1(z,z_0) = \text{Im}\,[Q_1(z,z_0)],\quad F_2(z,z_0) = \text{Re}\,[Q_2(z,z_0)-Q_1(z,z_0)]$$

$$Q_1(z,z_0) = \frac{\bar{z}(z+2z_0-3\bar{z}_0)+2z\bar{z}_0-(z_0-\bar{z}_0-z)(z+\bar{z}_0)}{(z-\bar{z}_0)^3}$$

$$Q_2(z,z_0) = \frac{2(z-\bar{z}_0)(2\bar{z}_0-z_0-z)}{(z-\bar{z}_0)^3}.$$

The singular term in H_c is interpreted in the Cauchy principal value sense.